Global ENA observations of the storm mainphase ring current: Implications for skewed electric fields in the inner magnetosphere

P. C:son Brandt,[1] S. Ohtani,[1] D. G. Mitchell,[1] M.-C. Fok,[2] E. C. Roelof,[1] and R. Demajistre[1]

Received 18 March 2002; revised 17 June 2002; accepted 19 July 2002; published 18 October 2002.

[1] The local time distribution of the ring current in the 27–119 keV range during several geomagnetic storm main phases have been investigated. The data was obtained by the high energy neutral atom (HENA) imager onboard IMAGE. Global proton distributions are derived from the observed energetic neutral atom (ENA) images using a linear inversion technique. During storms with low IMF B_y the peak of the proton distribution is around 01 MLT. For storms with high IMF B_y the peak can rotate to dawn. The rotation angle depends on solar wind velocity and interplanetary magnetic field (IMF) B_y, but less on IMF B_z. We discuss how this morphology implies the existence of strong and skewed equatorial electric fields in the inner magnetosphere. Our results are consistent with in-situ ring current measurements, radar observations and with kinetic models that self-consistently calculate the electric field produced by the closure of the partial ring current. *INDEX TERMS:* 2730 Magnetospheric Physics: Magnetosphere—inner; 2778 Magnetospheric Physics: Ring current; 2788 Magnetospheric Physics: Storms and substorms; 2740 Magnetospheric Physics: Magnetospheric configuration and dynamics; 2736 Magnetospheric Physics: Magnetosphere/ionosphere interactions. **Citation:** C:son Brandt, P., S. Ohtani, D. G. Mitchell, M.-C. Fok, E. C. Roelof, and R. Demajistre, Global ENA observations of the storm mainphase ring current: Implications for skewed electric fields in the inner magnetosphere, *Geophys. Res. Lett.*, *29*(20), 1954, doi:10.1029/2002GL015160, 2002.

1. Introduction

[2] The electric field of the inner magnetosphere is one of the most important features in understanding the development of the storm-time ring current. The magnetospheric electric field was believed to consist of the convectional (solar wind induced) dawn to dusk field and the corotaional field of the Earth. Therefore, ions were expected to $\mathbf{E} \times \mathbf{B}$ drift from the tail, around dusk and then out the dayside magnetopause during mainphases of geomagnetic storms. In this simple picture they would achieve their highest energy, and therefore highest flux, around dusk.

[3] Comparisons between observations and ring current models with fixed electric field models have implied an offset in local time for the electric field pattern about 2–3 hours [*Baumjohann et al.*, 1985; *Kistler et al.*, 1989; *Jordonova et al.*, 1998; *Fok et al.*, 1996]. Kinetic models have been constructed where the electric field is calculated self consistently, that is, the models calculate the electric field created by the closure of the partial ring current through the ionosphere [*Harel et al.*, 1981; *Fok et al.*, 2001; *Ridley and Liemohn*, 2002]. The results of these models suggest an eastward skewing of the electric field pattern. Furthermore, electric field measurements by Combined Release and Radiation Effects Satellite (CRRES) reveal strong (6 mV/m) electric fields at $L < 5$ [*Wygant et al.*, 1998]. It is also known that the high positive values of interplanetary magnetic field (IMF) B_y causes the ionospheric potential pattern to skew in local time [*Weimer*, 1995], but it is still unclear how this effects the equatorial ring current distribution.

[4] The high energy neutral atom (HENA) imager onboard the IMAGE spacecraft has imaged the ring current in the 10–200 keV range since May 2000. In all of the storm main phases the peak fluxes have originated from the midnight to dawn sector, consistent with the self-consistent models and the CRRES electric field measurements.

[5] In this paper we show that the eastward rotation of the peak of the ring current ion distribution depends on IMF B_y and solar wind velocity for high values of B_y. For lower values of IMF B_y, the rotation appears to depend more on solar wind velocity. We present examples of the global ion distributions in the 27–39 keV and 119–198 keV energy range showing significant eastward rotation over the entire energy range implying that the electric fields in the inner magnetosphere can be ~10 mV/m. The ion distributions are derived from the observed ENA images through a constrained linear inversion technique reported by *C:son Brandt et al.* [2002].

2. Global Ring Current Observations

[6] Table 1 lists the times of the storm main phases that are investigated in this paper. In the first three columns we show the times of observation, in the next three we show the IMF B_y, B_z and solar wind velocity v_x in geocentric solar ecliptic (GSE) coordinates. In the last column we show the local time position of the peak ion flux to within one hour accuracy. The solar wind data are 5-min averages and was taken from the ACE spacecraft and has been lagged for the arrival at Earth. Our goal for data selection was to obtain a data set where we could examine how the ring current responded during extended periods of enhanced magnetospheric convection, i.e. during long (~3 h) periods of negative IMF B_z. Therefore the selected events had to fullfill three requirements: (1) The minimum $Dst \leq -50$ nT for the storm; (2) The period of southward IMF had to be

[1]The Johns Hopkins University Applied Physics Laboratory, Laurel, MD, USA.
[2]NASA Goddard Space Flight Center, USA.

0094-8276/02/2002GL015160$05.00

Table 1. Times of observations, 5-min averaged solar wind parameters in GSE coordinates and the MLT location of the maximum ion flux (27–39 keV)

Year	DOY	UT	B_y (nT)	B_z (nT)	v_x (km/s)	MLT (h)
2000	224	04:59	7	−10	434	04
2000	225	09:41	31	−13	618	05
2000	256	10:58	6	−7	352	23
2000	274	13:53	11	−3	410	01
2000	278	18:02	4	−12	417	03
2000	288	08:20	5	−7	383	02
2000	303	03:28	9	−14	405	03
2000	333	22:57	−5	−5	544	00
2000	358	05:48	5	−11	309	00
2001	079	11:00	−5	−17	393	00
2001	275	08:20	−2	−8	369	01
2001	276	11:29	1	−20	523	01
2001	294	18:54	25	−8	650	04
2001	305	12:16	10	−6	338	23
2002	083	14:24	−12	−3	434	01
2002	108	10:28	−8	−11	481	02
2002	109	17:09	−9	−8	519	03
2002	110	05:39	1	−5	648	01

at least ~3 h long; (3) The IMAGE vantage point had to be nearly over the north pole, so that the local time distribution of the ions could be well resolved. During each north-pole passage of the IMAGE spacecraft, no significant change in the local time distribution could be detected. Each passage offers good viewing over the local time distribution for about 3–6 hours. We stress that the lack of motion of the peak in local time does not imply that the plasma is stagnated. See the Discussion section for a more detailed discussion about the implications.

[7] Figure 1 shows a typical example of a proton distribution from the main phase during the 4 October 2000 storms. The proton distributions were retrieved from the ENA images by using the constrained linear inversion technique described by *C:son Brandt et al.* [2002]. This technique assumes a dipolar magnetic field, but since we are focused on the L < 5 ring current we expect no large errors. This morphology is set up early in the main phase and remains the same as long as the IMF B_z remains negative.

[8] We define the skewing angle as the angle between the peak of the ion distribution and local midnight, positive angles in the anti clockwise direction viewed from above the north pole. In Figure 2a–2c we show three plots of the skewing angle for the 27–39 keV proton distribution as a function of IMF B_y, IMF B_z, and solar wind velocity v_x. We calculated the correlation coefficients for all events (open and filled circles of a total of 18 events) and for events with IMF $B_y \leq 5$ nT (9 events shown by open circles). The correlation coefficients for all events are listed below each figure and the coefficients of the events restricted to IMF $B_y \leq 5$ nT are listed in parentheses. For all events the 27–39 keV proton distribution peaked on average around 01:30 MLT, and for the IMF B < 5 nT the peak was located around 01:00 MLT. We see that for all events both IMF B_y and v_x appears to govern the skewing. For storms with low IMF B_y, the correlation with all quantities decreases and the statistical spread increases. Although there is a general trend in Figure 2b, the correlation with IMF B_z was surprisingly low for both cases. A closer look at Figure 2c reveals two possible branches (open and closed circles). The branch for IMF $B_y \leq 5$ nT (open circles), whereas the branch for IMF $B_y > 5$ nT (filled circles) have the same trend but appears to be shifted towards higher skewing angles. For the 81–119 keV range the peak was located around 23:30 MLT for both B_y cases. The corresponding correlation coefficients were not above 0.3. We stress that more studies are needed before any accurate conclusion can be drawn.

3. Discussion

[9] Models of the ring current that self-consistently calculate the electric field produced by the closure of the

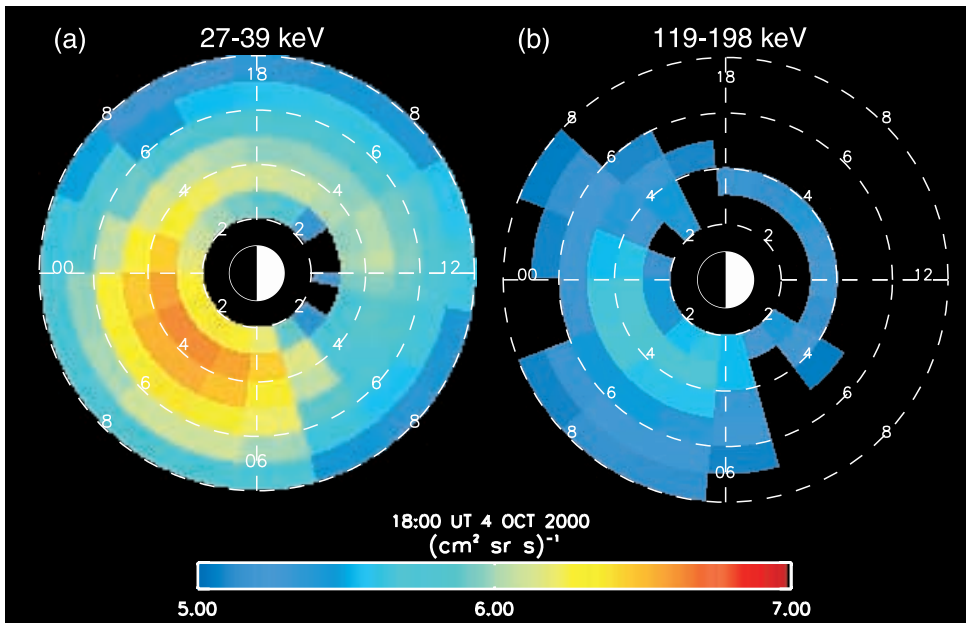

Figure 1. Examples of the proton distributions obtained by inverting the ENA images using a constrained linear inversion technique [*C:son Brandt et al.*, 2002]. The mainphases of 4 October 2000 storm for (a) 27–39 keV and (b) 119–198 keV.

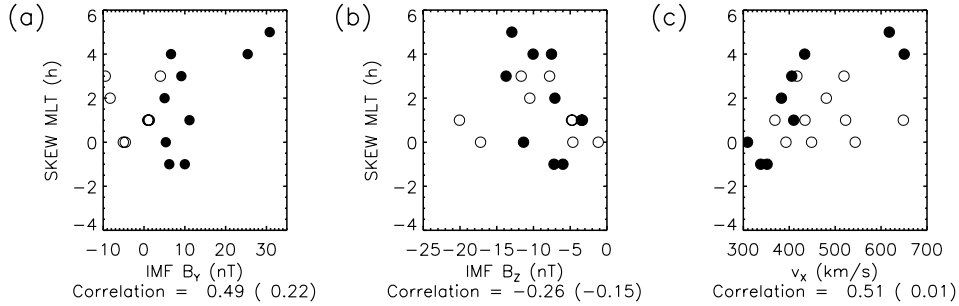

Figure 2. Plot showing the correlation between skew angle of the peak of the proton distribution and the (a) the IMF B_y, (b) IMF B_z, and (c) solar wind velocity v_x. Open circles represent events where IMF $B_y \leq 5$ nT and filled circles where IMF $B_y > 5$ nT. Correlation coefficients for open circles are listed in parentheses.

region 2 current system, reproduce an eastward skewing and enhancement of the electric field [*Wolf*, 1983; *Fok et al.*, 2001; *Ridley and Liemohn*, 2002]. Both the model results and our observations are supported by observations of unexpectedly strong electric fields in the inner magnetosphere and the low-latitude ionosphere. *Wygant et al.* [1998] reported observations of electric fields during magnetic storms up to 6 mV/m at L = 2–4 measured by the CRRES satellite. Fast ionospheric ion flows have been observed by the Millstone Hill Radar facility which imply ionospheric electric field strength 60 mV/m at <50° MLAT (Personal communication J. Foster, MIT, Haystack Observatory, MA).

[10] The observed skewing for high energies can lead us to some important conclusions about the strength of the electric field in the inner magnetosphere. Figure 1 shows the proton distribution up to 119–198 keV. Although no space to report it in detail here, we investigated the skewing up to 198 keV, and in general the skewing was less severe. For the 81–119 keV range the peak of the ion distribution was located at 23:30 MLT. If the electric field is strong (low ion energy) ions will be moving along the equipotentials. If the magnetic drift is strong (ion energy high) ions will have their closest approach to Earth at around dusk and achieve their highest energy (and therefore highest flux) there. Now, the fact that the skewing extends significantly over energy suggests that the electric field is strong enough so that the $\mathbf{E} \times \mathbf{B}$ drift can compete with the magnetic drift. For example, in a 10 mV/m electric field an equatorially mirroring 100 keV proton at L = 4 (dipole) will experience an $\mathbf{E} \times \mathbf{B}$ drift velocity comparable to the magnetic gradient drift velocity.

[11] Although our study suggests that there is an additional eastward skewing related to high positive IMF B_y values it is not known how the IMF B_y relates to the equatorial electric field of the inner magnetosphere and how it effects the development of the storm-time ring current. However, it is interesting to note that high positive values of IMF B_y skew the high-latitude ionospheric potential pattern [*Weimer*, 1995]. The reason for this is believed to be related to the location of the merging lines on the dayside magnetopause [*Khurana et al.*, 1996].

[12] These findings imply that a new picture of the build-up of the storm main phase ring current may emerge. The skewed and strong electric fields of the inner magnetosphere suggest that ions are transported in to the post midnight sector and exit through the dusk or afternoon magnetopause. A more detailed study is currently being pursued and will be submitted to *Journal of Geophysical Research*.

[13] **Acknowledgments.** Our thanks to the ACE science and data processing team for providing solar wind data.

References

Baumjohann, W., G. Haerendel, and F. Melzner, Magnetospheric convection observed between 0600 and 2100 LT: Variations with *Kp*, *J. Geophys. Res.*, *90*, 393–398, 1985.

C:son Brandt, P., R. Demajistre, E. C. Roelof, D. G. Mitchell, and S. Mende, IMAGE/HENA: Global ENA imaging of the plasmasheet and ring current during substorms, *J. Geophys. Res.*, in press, 2002.

Fok, M. C., T. E. Moore, and M. E. Greenspan, Ring current development during storm main phase, *J. Geophys. Res.*, *101*, 15,311–15,322, 1996.

Fok, M. C., R. A. Wolf, R. W. Spiro, and T. E. Moore, Comprehensive computational model of Earth's ring current, *J. Geophys. Res.*, *106*, 8417–8424, 2001.

Harel, M., R. A. Wolf, P. H. Reiff, R. W. Spiro, W. J. Burke, F. J. Rich, and M. Smiddy, Quantitative simulation of a magnetospheric substorm 1. Model logic and overview, *J. Geophys. Res.*, *86*, 2217–2241, 1981.

Jordonova, V. K., et al., October 1995 magnetic cloud and accompanying storm activity: Ring current evolution, *J. Geophys. Res.*, *103*, 79–92, 1998.

Khurana, K. K., R. J. Walker, and T. Ogino, Magnetospheric convection in the presence of interplanetary magnetic field B_y: A conceptual model and simulations, *J. Geophys. Res.*, *101*, 4907–4916, 1996.

Kistler, L. M., F. M. Ipavich, D. C. Hamilton, G. Gloeckler, B. Wilken, G. Kremser, and W. Stüdemann, Energy spectra of the major ion species in the ring current during geomagnetic storms, *J. Geophys. Res.*, *94*, 3579–3599, 1989.

Ridley, A. J., and M. W. Liemohn, A model-derived stormtime asymmetric ring current driven electric field description, *J. Geophys. Res.*, in press, 2002.

Weimer, D. R., Models of high-latitude electric potentials derived with a least error fit of spherical harmonic coefficients, *J. Geophys. Res.*, *100*, 19,595–19,607, 1995.

Wolf, R., *Solar Terrestrial Physics*, pp. 303–368, D. Reidel, Hingham, MA, 1983.

Wygant, J., D. Rowland, H. J. Singer, M. Temerin, F. Mozer, and M. K. Hudson, Experimental evidence on the role of the large spatial scale electric field in creating the ring current, *J. Geophys. Res.*, *103*, 29,527–29,544, 1998.

P. C:son Brandt, S. Ohtani, D. G. Mitchell, M.-C Fok, E. C. Roelof, and R. Demajistre, The Johns Hopkins University, Applied Physics Laboratory, 11100 Johns Hopkins Rd., Laurel, MD 20723-6099, USA.